A Non-Local Diffusion Saliency Model for Magnetic Resonance Imaging

I. Ramírez[1], G. Galiano[2], N. Malpica[1] and E. Schiavi[1]
[1]*Dpt. of Applied Mathematics, Material Sciences and Electronic Technology, King Rey Juan Carlos University, C/Tulipán s/n, 28933, Móstoles, Madrid, Spain*
[2]*Dpt. of Mathematics, Oviedo University. c/ Calvo Sotelo, 33007-Oviedo, Spain*

Keywords: Saliency Detection, Segmentation, Non-local Diffusion, Non-convex Optimization, Bilateral Filtering, P-laplacian Operator, MRI, FLAIR, Tumor, Edema.

Abstract: Based on previous work on image classification and recent applications of non-local non-linear diffusion equations, we propose a non-local p-laplacian variational model for saliency detection in digital images. Focusing on the range $0 < p < 1$ we also consider the regularized non-convex fluxes generated by the related hyper-laplacian diffusion operators. With the aim of exploring the properties and potential applications of such non-local, non-convex operators the model is applied to Magnetic Resonace Imaging (MRI) for Fluid Attenuated Inversion Recovery image (FLAIR) modality showing promising numerical results. In this work Saliency shall be understood as the relevant, outstanding region in a FLAIR image, which is commonly the brightest part. It corresponds to a tumor and neighborhood edema. Our preliminary experiments show that the proposed model can achieve very accurate results in this modality in terms of all the considered metrics.

1 INTRODUCTION

There is a general, growing interest in digital image processing and computer vision applications for (Visual) Saliency based models able to focus on perceptually relevant information in digital images. Semantic segmentation, object detection, object proposals, image clustering, retrieval and cognitive saliency applications such as image captioning and high-level image understanding are just few examples of saliency based models. Saliency is also of interest as a means to improve computationally efficiency and increases robustness to clustering and threshold. Despite the lack of a general consensus on a proper mathematical definition of Saliency, it has a biologically perceptive meaning whereas it models the mechanism of human attention and consists of the task of finding interesting objects in an image with or without prior knowledge. It turns out that the right role of saliency in models is then application dependent and this limit the scope of general purpose methods. Recently there is been a burst of research on Saliency due to its wide application in leading medical disciplines such as Neuroscience and Cardiology. In fact, when considering medical images such as those acquired in Magnetic Resonance Imaging (MRI) or Positron Emission Tomography (PET), the automatic obtainment of saliency maps, can be useful for pathology detection, disease classification (Rueda et al., 2013), location and segmentation of brain strokes, gliomas, myocardium detection for PET images, tumors quantification in FLAIR MRI (Thota et al., 2016) etc. Several different techniques and approaches have been applied to construct saliency maps. They vary from low dimensional manifold features minimization (Zhan, 2011), non-local sparse minimization (Wang et al., 2014), graphs techniques (Harel et al., 2006), Partial Differential Equations (PDE) (Li et al., 2013), superpixel (Liu et al., 2013), learning (Liu et al., 2014) and Neural Networks based approaches (Bylinskii et al.,) (MIT-Benchmark).

With the aim to explore the applications and algorithms of non-smooth, non-local, non-convex optimization to PDE saliency based models, we present in these notes, a new non-Local diffusion model for PDE applied to Fluid Attenuated Inversion Recovery (FLAIR) MR images for accurate location of tumor and edema. The basis for the modeling exercise relies in a recent model proposed by Li (Li et al., 2013) for natural images saliency detection. Recent results which justifies the interest for this applications can be found in (Thota et al., 2016) and multichannel pseudo RGB (Banerjee et al., 2016). PDE based variational methods have provided to be effective to model general low level computer vision processing tasks (denoising, restoration, deblurring, segmentation, super-

RamÃ■rez I., Galiano G., Malpica N. and Schiavi E.
A Non-Local Diffusion Saliency Model for Magnetic Resonance Imaging.
DOI: 10.5220/0006172101000107
In *Proceedings of the 10th International Joint Conference on Biomedical Engineering Systems and Technologies (BIOSTEC 2017)*, pages 100-107
ISBN: 978-989-758-215-8

resolution) allowing specific solutions to be obtained based on Bayesian modelling. When first order necessary optimality conditions are imposed on the non-linear energy functional modeling data and *a priori* knowledge, a PDE arises which has to be numerically solved. Primal gradient-descent is a first step for a problem understanding. Alternatively non-linear diffusion processing has been shown to be a valid filtering data processing method to design specific preprocessing steps for further analysis. In any case, we are leaded to solve non-linear (local) parabolic diffusion equations. Anisotropy is an important characteristic which can also be modeled in such a local flux based diffusive processes, (Weickert, 1998). Nevertheless, when non-local interactions are important for pathology detection, non-local diffusion equations have to be considered. Non-local integro-differential equations have a long history, since the Fredholm integral equations of the first kind, but a great deal of interest has been recently triggered due to its applications in image processing (Gilboa and Osher, 2008).

Based on such arguing we propose to extend the local $p-$laplacian classification model of (Samson et al., 1998) to a non-local framework for saliency detection, and the non-local model proposed by (Li et al., 2013) for $p > 2$ to include non-convex fluxes related to the range $0 < p < 1$. This paper is organized as follows. In section (2), based on the approach of (Samson et al., 1998) for image classification, we define a local variational model which includes a new term for saliency detection. It generates an absorption-reaction balance which drives the diffusion process promoting a two classes binary image labeling. Remarkably, such a term has a concave energy leading to a fast saliency detection. We also define an approximating family of edge-preserving potential functions which allows to describe non-convex diffusive fluxes. In section (3) we introduce the non-local framework for PDE (Andreu-Vaillo et al., 2010). Based on the approach of (Li et al., 2013), we define a new variational model with the non-local p-laplacian operator that provides non-local diffusion, combined with a fidelity term coming from the Restoration Bayesian framework, and a saliency term, inspired by the Ginzburg-Landau (Aubert et al., 2005) superconductor theory. Non-local diffusion has multiple applications in the literature among which stands out the detection and preserving patterns capacity. However, when non-local non-convex flux is acting, the non-convexity imposed (as *a priori* knowledge) with $0 < p < 1$, forces the non-local gradient to be *sparse*, in so far it minimizes the number of jumps (big non-local gradient modulus) in the image domain. Actually, only sharp jumps are preserved, and the resulting image looks like a cartoon piece-wise constant image. In section (4) we describe the numerical discretization using a semi-implicit Euler scheme combined with a quantization step to speed up the computations (Yang et al., 2009). The final saliency mask is finally computed by a simple thresholding step. A mask is generated to compare with the ground-truth. Finally, in section 5 we present some preliminary results which show the promising performance of the model in terms of accuracy and speed when applied to FLAIR sequences of MR images.

2 LOCAL DIFFUSION EQUATIONS

We start with a Bayesian Restoration model for image classification which produces a Maximum a Posteriori (MAP) estimation of the solution through the minimization of a nonlinear energy functional in $\Omega \subset \mathbb{R}^2$. Let λ and α be fixed positive parameters. We consider the functional (Samson et al., 1998)

$$E_{\varepsilon,p}(u) = \alpha J_{\varepsilon,p}(u) + \frac{1}{\alpha} H(u) + \lambda F(u) = \quad (1)$$

$$= \alpha \int_\Omega \phi_{\varepsilon,p}(|\nabla u|)\, dx + \frac{1}{\alpha}\int_\Omega h(u) dx + \\ + \frac{\lambda}{2}\int_\Omega |Ru - f|^2\, dx$$

where $h(u)$ is typically a quadratic function known as a double-well potential function which we shall precise later on. The functions

$$\phi_{\varepsilon,p}(s) = \frac{2}{p}\left(s^2 + \varepsilon^2\right)^{p/2} - \frac{2}{p}\varepsilon^p \quad (2)$$

define an approximating family that allows to overcome the no differentiability when $0 < p \leq 1$. When $\varepsilon \to 0$ we have $\phi_{\varepsilon,p}(s) \to \phi_{0,p}(s) = (2/p)|s|^p$. When $\varepsilon > 0$ the $\phi_{\varepsilon,p}$ family is differentiable for any p and non-convex for $0 < p < 1$. In fact, it is concave except at a thin layer of thickness ε near the origin (see Figure 1). Despite of the non convexity, the $\phi_{\varepsilon,p}$-family is edge-preserving (Charbonnier et al., 1997). This family satisfies $\phi_{\varepsilon,p}(0) = 0$ for any p, ε. We shall assume $0 < p \leq 1$ and $\varepsilon > 0$. We have

$$\phi'_{\varepsilon,p}(s) = 2s\left(s^2 + \varepsilon^2\right)^{(p/2)-1},$$

and then $\phi'_{\varepsilon,p}(0) = 0$ for any p, ε and $\phi'_{\varepsilon,p}(s) > 0$ for $s > 0$ and $\forall p, \varepsilon$. When $h(u) \equiv 0$ the following results are well known. For parametric values $p > 1$ the energy $E_{\varepsilon,p}(u)$ defined in (1) is convex and differentiable presenting a unique global minimum. The diffusive local flux over-smooths the solutions and blurs

the edges. For $p = 1$ and $R \equiv I_d$ we recover the celebrated ROF model (Rudin et al., 1992). The energy is convex but no differentiable. We have again a unique global minimum (Chambolle and Lions, 1997) in a weak sense, say $L^\infty(\Omega) \cap BV(\Omega)$, where $BV(\Omega)$ is the space of Bounded Variation Functions. This space includes discontinuous functions and its gradient is a Bounded Radon measure. Details on the geometric measure theory underlying this notions can be found in the book of (Ambrosio et al., 2000).

Notice that when functionals like (1) are used for image classification, partitioning and labeling, the set of functions on which we minimize (for example, piece-wise constant binary functions taking values $\{0,1\}$) is not convex and the overall minimization problem is not convex despite of the convexity of the energy functional. Moreover, as shown in (Samson et al., 1998), the solutions need not to be piecewise constant for $\alpha > 0$, and this suggests to look for solutions in the closed, convex interval $[0,1]$. When $\alpha \to 0$ the Γ-convergence theory (so far proved only for $p > 1$) assures the existence of piece-wise constant binary solutions.

For $0 < p < 1$ the energy is non-convex (in fact concave) and non-smooth. No much is known theoretically in this range because the functional is not differentiable and we are working with the so called $p-$quasi-norms of the $L^p(\Omega)$ spaces and the direct method of variational calculus cannot be applied anymore. The problem lacks of a sound mathematical theory. A differential approximation is in order to get insight into the numerical behavior of its solutions. Let $|\nabla u|_\varepsilon^2 = |\nabla u|^2 + \varepsilon^2$. The associated Euler-Lagrange equation is

$$-\alpha \mathrm{div}\left(\frac{\phi'_{\varepsilon,p}(|\nabla u|)}{|\nabla u|_\varepsilon}\nabla u\right) + \frac{1}{\alpha}h'(u) + \lambda R^*(Ru - f) = 0 \quad (3)$$

for $p > 0$, $\lambda > 0$ fixed and $f \in L^\infty(\Omega)$ given. If $p > 1$ we can set $\varepsilon = 0$ and no regularization of the diffusion operator takes place. For $p = 1$ the $1-$Laplacian operator is considered and duality arguments (Chambolle, 2004) have to be invoked to properly solve the *exact* (not $\varepsilon-$approximating) TV minimization problem. For $0 < p < 1$ the problem is open even with $h(u) = 0$. Remarkably, Hintermüller has recently shown the existence of a *viscosity solution* (Hintermüller and Wu, 2014). The term $h'(u)$ we propose for saliency detection is a simple linear functional given by

$$h'(u) = \delta(1 - \delta u) \quad (4)$$

which is the Frechet differential of the function

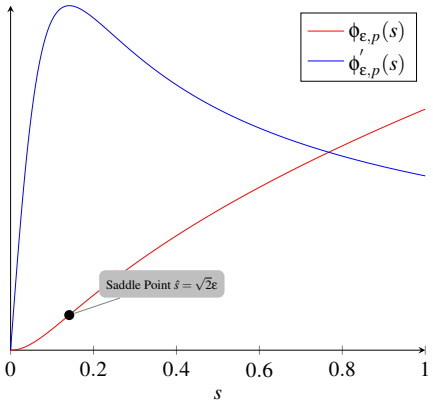

Figure 1: A plot of a member of the $\phi_{\varepsilon,p}$ family. The saddle point defines the transition from the convex initial layer to a concave profile.

$$h(u) = -\frac{1}{2}(1 - \delta u)^2 \quad (5)$$

where δ is a real positive parameter which can be conveniently fixed to deal with the variability of natural images. Contrary to the common usage of *convex* quadratic terms to model *double-well* for image classification (Aubert and Kornprobst, 2006), we propose in (5) a *concave* quadratic energy term

$$H(u) = \int_\Omega h(u)dx = -\frac{1}{2}\int_\Omega (1 - \delta u)^2$$

In fact, the minimum of $h(u)$ when $u \in [0,1]$ is

$$\min_{u\in[0,1]} h(u) = \min\{h(0), h(1)\} = m$$

where $m = h(0)$ for $0 < \delta < 2$, $m = h(0) = h(1)$ for $\delta = 2$ and $m = h(1)$ for $\delta > 2$. In any case, the minimum m is attained at the boundary of the interval $[0,1]$, which are the labels we impose for saliency detection (foreground) $u = 1$, and $u = 0$ for background. The term $H(u)$ promotes the detection of salient regions of interest (foreground) separated by regions with no relevant information (background) while keeping the edges and details of the given data image $f \in L^\infty(\Omega)$ thanks to the *edge-preserving* properties of the $\phi_{\varepsilon,p}$-family.

Finally, the fidelity term $F(u)$ models image restoration and can be used to perform joint reconstruction, deconvolution, super-resolution, denosing of the given data. In the application we are concerned with we simply set $R \equiv I_d$.

The Euler-Lagrange equation (3) is complemented, as usual in image processing, with homogeneous Neumann boundary conditions on $\partial\Omega$. Using a gradient descent we are leaded to

$$u_t = \alpha \mathrm{div}\left(\frac{\phi'_{\varepsilon,p}(|\nabla u|)}{|\nabla u|_\varepsilon}\nabla u\right) + \frac{\delta}{\alpha}(\delta u - 1) - \lambda(u - f) \quad (6)$$

which is for $p > 1$ the classical $p-$laplacian diffusion operator

$$u_t = \alpha \Delta_p u + \frac{\delta}{\alpha}(\delta u - 1) - \lambda(u - f) \quad (7)$$

The lower order r.h.s term models a linear absorption-reaction balance which can produce different asymptotic behaviors depending on the chosen parametric values. In fact we have

$$\frac{\delta}{\alpha}(\delta u - 1) - \lambda(u - f) =$$
$$= \left(\frac{\delta^2}{\alpha} - \lambda\right) u + \left(\lambda f - \frac{\delta}{\alpha}\right) = au + b$$

Typical values used in the simulation, $\lambda \approx 0.1$, $\alpha \approx 0.5$, $\delta \approx 2$, $\rho \approx 20$, give $a \approx 7.9$ and $b \approx -3.9$. As a result, the linear term $au + b$ models absorption when u is positive and small, say $u \approx 0$ (background), and it acts as a reaction term in the region where $u \approx 1$ (foreground). This mechanism pushes the solution toward the labels of the two classes allowing a simple threshold for the final binary mask targeting the ground-truth image.

3 NON-LOCAL DIFFUSION EQUATIONS

We first briefly introduce the mathematical framework of Andreu et al. which defines, for $1 \leq p \leq +\infty$ the non-local p-laplacian diffusion operators. Then, in the framework of bilateral filtering, we extend the filter to include diffusion parameters $0 < p < 1$. We start with considering flux functions $\phi_p(s) = (2/p)|s|^p$ for non-local diffusion. For $p > 1$ they are strictly convex and differentiable, for $p = 1$ we have a convex, sub-differentiable function and for $0 < p < 1$ we are not aware of any mathematical result about existence of variational solutions. Nevertheless many papers report on the improved numerical performance of non-convex functions in terms of quality and numerical efficiency. This has been observed in the local framework where these functions are considered, when $0 < p < 1$, as *edge-preserving functions*. In the non-local case this is, so far, unexplored.

3.1 Non-local Strictly Convex Flows

This corresponds to $\phi_{\varepsilon=0,p}(s) = \phi_p(s) = (2/p)|s|^p$, with $p > 1$. The non-local analogous of the p-laplacian operator $\Delta_p u$ is given by

$$DJ_p^{NL}(u) = \frac{1}{4}\int_\Omega w(x-y)\phi'_p(u(y) - u(x))dy = \quad (8)$$
$$= \int_\Omega w(x-y)|u(y) - u(x)|^{p-2}(u(y) - u(x))dy$$

which is the Frechet derivative (for $p > 1$) of

$$J_p^{NL}(u) = \frac{1}{2p}\int_{\Omega\times\Omega} w(x-y)\phi_p(u(y) - u(x))dydx = \quad (9)$$
$$= \frac{1}{2p}\int_{\Omega\times\Omega} w(x-y)|u(y) - u(x)|^p dydx$$

As typical in bilateral filtering theory (Tomasi and Manduchi, 1998) we define the $w(x-y)$ function in form

$$w(x-y) = \left(\frac{1}{C}\right) e^{-\frac{(|x-y|)^2}{\rho^2}}, \quad (x,y) \in \Omega \times \Omega$$

where C is a normalizing constant.

While the corresponding local case is not to much relevant to the image processing community because of its regularizing effect on the solutions which provokes artificial smoothing due to elliptic regularity theory, there is an important result of (Andreu-Vaillo et al., 2010) which assures that, for the related non-local diffusion case, the data and the solution space are the same and no regularization takes efect. This intriguing effect is due to non-local diffusion and can be related to recent bilateral filter theory and application.

3.2 Approximating Non-local Non-convex Flows

When $0 < p \leq 1$ we use the already presented $\phi_{\varepsilon,p}-$family (2). Denote $x \in \Omega$ as a pixel in the image and $y \in \Omega$ as a pixel in the neighborhood $N(x)$ of x, $u(x)$ and $u(y)$ as the corresponding range values of pixel x and y. We consider the functional

$$J_{\varepsilon,p}^{NL}(u) = \frac{1}{4}\int_{\Omega\times\Omega} w(x-y)\phi_{\varepsilon,p}(u(y) - u(x))dxdy = \quad (10)$$
$$= \frac{1}{2p}\int_{\Omega\times\Omega} w(x-y)\left(|u(y) - u(x)|^2 + \varepsilon^2\right)^{p/2} dxdy +$$
$$-\frac{\varepsilon^p}{2p}\int_{\Omega\times\Omega} w(x-y)dxdy$$

When $u \equiv 0$ we have $u(y) = u(x)$ for any $x, y \in \Omega$ and $J_{\varepsilon,p}(0) = 0$. In the limit

$$\lim_{\varepsilon\to 0} J_{\varepsilon,p}(u) = J^{NL}_{0,p}(u) =$$

$$= \frac{1}{2p}\int_{\Omega\times\Omega} w(x-y)|u(y)-u(x)|^p dxdy$$

which is the non-local analogous of to the energy functional associated to the local p-laplacian operator

$$E_p(u) = \frac{1}{p}\int_\Omega |\nabla u|^p dx$$

as before the derivative of the approximated non-local functional (10) can be formally written as

$$DJ^{NL}_{\varepsilon,p}(u) = \frac{1}{4}\int_\Omega w(x-y)\phi'_{\varepsilon,p}(u(y)-u(x))dy = \quad (11)$$

$$= \int_\Omega w(x-y)(|u(y)-u(x)|^2+\varepsilon^2)^{\frac{p-2}{2}}(u(y)-u(x))dy$$

Using the gradient descent method to minimize the functional $J_{\varepsilon,p}(u)$ we arrive at the evolution equation

$$u_t(x,t) = \frac{1}{2}\int_\Omega w(x-y)\phi'_{\varepsilon,p}(u(y,t)-u(t,x))dy$$

where

$$\phi'_{\varepsilon,p}(u(y,t)-u(x,t)) =$$

$$= \left(|u(y,t)-u(x,t)|^2+\varepsilon^2\right)^{\frac{p-2}{2}}(u(y,t)-u(x,t))$$

We define the kernel

$$k_{\varepsilon,p}(s) = \frac{1}{2}\phi'_{\varepsilon,p}(s) = s\left(s^2+\varepsilon^2\right)^{\frac{p-2}{2}}$$

and finally write

$$u_t(x,t) = K_{\varepsilon,p}(u)(x,t) = \quad (12)$$

$$= \int_\Omega w(x-y)k_{\varepsilon,p}(u(y,t)-u(x,t))dy$$

which is complemented with initial data $u(x,0) = u_0(x), x\in\Omega$. As remarked in (Andreu-Vaillo et al., 2010), the homogeneous Neumann boundary conditions are implicitly imposed by the non-local diffusion operator $K_{\varepsilon,p}$. The equation above models a nonlinear non-local non-convex $p-$laplacian bilateral filter. This will be used in the next section to present final joint model for saliency detection and restoration.

3.3 Proposed Model

We present the general model valid for non-local strictly convex flows ($\varepsilon = 0,\ p > 1$) and the approximated non-local non-convex flows ($\varepsilon > 0, 0 < p < 1$). We start with the analogous non-local energy functional

$$E_{\varepsilon,p}(u) = \alpha J^{NL}_{\varepsilon,p}(u) + \frac{1}{\alpha}H(u) + \lambda F(u) \quad (13)$$

Using the definitions introduced in section (2) regarding the saliency and the fidelity terms, we consider the energy functional $J^{NL}_{\varepsilon,p}(u)$ defined in (10). The non-local Euler Lagrange equation reads

$$-\frac{\alpha}{4}\int_\Omega w(x-y)\phi'_{\varepsilon,p}(u(y)-u(x))dy + \quad (14)$$

$$+\frac{1}{\alpha}h'(u) + \lambda(u-f) = 0$$

and the corresponding gradient flow evolution equation is

$$u_t = \frac{\alpha}{4}\int_\Omega w(x-y)\phi'_{\varepsilon,p}(u(y,t)-u(x,t))dy + \quad (15)$$

$$-\frac{1}{\alpha}h'(u) - \lambda(u-f)$$

which is in term of kernel $k_{\varepsilon,p}$ (12)

$$u_t = \frac{\alpha}{4}\int_\Omega w(x-y)k_{\varepsilon,p}(u(y,t)-u(x,t))dy + \quad (16)$$

$$-\frac{1}{\alpha}h'(u) - \lambda(u-f)$$

4 NUMERICAL RESOLUTION

We solve the non-local p-laplacian diffusion equation (16) using the approach proposed in (Yang et al., 2009). This is based on the quantization process which allows to reduce diffusion term to a convolution operation over each quantized value. In fact, this technique produces solutions in a quantized range of values which is suitable for our proposal which is to separate and detecting saliency ($u \approx 1$) from background ($u \approx 0$). Such technique allows to speed up the bilateral non-local filtering and labeling. We then address the main saliency detection problem with a primal gradient descent numerical scheme.

4.1 Iterative Scheme

We briefly describe the quantization step which linearizes the model Let $q = (q_i)$ be a quantized vector, $q \in \mathbb{R}^Q$, where Q is the number of quantization levels and $q_i \in \{0,...,1\}$ are the *quantized* values. Moreover we denote $u_k(x) = u(x,t)$ for $t^k \in [(k-1)\Delta t, k\Delta t)$ and then $K_{\varepsilon,p}(u)(x,t) = K_{\varepsilon,p}(u_k)(x)$. For $k = 0$ we define a quantized version of the given data $u(x,0) = u_0(x) \in \{0,...,1\}$. Notice that the original FLAIR images we consider have a 16 depth-bit resolution which gives 65536 possible gray levels. For computational purposes we reduce the date image to a 8 depth-bit resolution corresponding to 256 values. This fix the number of quantization levels $Q = 256$ and allows the

exact computation of the reconstructed quantized solution. For each q_i, $i = 1..Q$ we introduce and compute the functions

$$K^i_{\varepsilon,p}(u_k(x)) = (k_{\varepsilon,p}(u_k - q_i) * w)(x) =$$

$$= \int_\Omega w(x-y) k_{\varepsilon,p}(u_k(y) - q_i) dy =$$

$$= \int_\Omega w(x-y)(|u_k(y) - q_i|^2 + \varepsilon^2)^{\frac{p-2}{2}} (u_k(y) - q_i) dy$$

where $K^i_{\varepsilon,p}(u_k) = k_{\varepsilon,p}(u_k - q_i) * w$ is a convolution operator. The contribution of each q_i is then summed up recover the effect of diffusion at any $x \in \Omega$. For any x such that $u_k(x) = q_i$ we define $F(u(x))$ as follows

$$F_i(u_k(x)) = \begin{cases} K^i_{\varepsilon,p}(u_k(x)), & \text{if } u_k(x) = q_i \\ 0, & \text{otherwise} \end{cases}$$

so that

$$F(u_k(x)) = \sum_i F_i(u_k(x))$$

The above formalism leads to a semi-implicit scheme (for the sake of readability we write $u_k = u_k(x)$) using a first-order forward Euler time discretization in (16). We have

$$u_{k+1} = u_k + \Delta t \alpha F(u_k) - \Delta t \frac{\delta}{\alpha}(1 - \delta u_{k+1}) + \quad (17)$$
$$- \Delta t \lambda (u_{k+1} - f)$$

Rearranging terms we have the following explicit scheme. Given a data image f and parameters α, λ, δ we fix Δt and set $k = 0$, $u_0 = f$. For any $k = 1..T$ compute:

$$\left(1 - \frac{\delta^2}{\alpha} + \lambda \Delta t\right) u_{k+1} = u_k + \Delta t \left(\alpha F(u_k) + \lambda f - \frac{\delta}{\alpha}\right)$$

Notice that, as typical in bilateral filtering theory, the diffusion time T is small because of the non-local diffusion.

4.2 Results

Signal in MR images is high or low (bright or dark), depending on the pulse sequence used, and the type of tissue in the image region of interest. In this work we present our preliminary results obtained solving the model equation (16) when applied to a FLAIR set of images from the BRATS2015 dataset (Menze et al., 2014). For all tests we have fixed the parameters: $\lambda = 0.1$, $Q = 256$, $\rho = 20$, $\alpha = 0.5$, $\varepsilon = 1e-6$, and for each image $1,2,3,4$, we choose $\delta = 2, 1.5, 2.5, 1.5$ respectively. The parameters of the numerical discretization are summarized in table (1), where Δt is the time discretization step, $T = k\Delta t$ corresponds to the total diffusion time and k is the number of iterations. The results are summarized in table (2) where we used the typical statistics and performance metrics for saliency and segmentation: Accuracy, Sensitivity, Specificity, G-mean, Precision, Recall and DICE. In all cases the results are very promising and show the successful application of the method, as indicated by the DICE coefficient, is associated to small values of p. In the non-convex case, the Precision is higher than the Recall, and in the convex case it is exactly the opposite. The accuracy is in all cases extremely high.

Table 1: Numerical parameters of the simulation.

	p = 0.1	**p = 0.5**	**p = 1**	**p = 2**	**p=3**
Δt	0.0025	0.005	0.01	0.01	0.01
k	80	40	30	20	20
T	0.2	0.2	0.3	0.4	0.4

Table 2: Statistics for different values of p.

p = 0.1	**Image**	**Precision**	**Recall**	**DICE**
	1	0,959	0,916	0,937
	2	0,964	0,909	0,936
	3	0,984	0,876	0,927
	4	0,973	0,887	0,928
	Average	0,970	0,897	0,932

p = 0.5	**Image**	**Precision**	**Recall**	**DICE**
	1	0,895	0,955	0,924
	2	0,935	0,915	0,925
	3	0,974	0,878	0,923
	4	0,938	0,920	0,929
	Average	0,935	0,917	0,925

p = 1	**Image**	**Precision**	**Recall**	**DICE**
	1	0,862	0,958	0,908
	2	0,911	0,919	0,915
	3	0,956	0,901	0,928
	4	0,932	0,932	0,932
	Average	0,915	0,928	0,921

p = 2	**Image**	**Precision**	**Recall**	**DICE**
	1	0,854	0,959	0,903
	2	0,868	0,924	0,895
	3	0,932	0,911	0,921
	4	0,898	0,935	0,916
	Average	0,888	0,932	0,909

p = 3	**Image**	**Precision**	**Recall**	**DICE**
	1	0,853	0,959	0,903
	2	0,835	0,930	0,880
	3	0,926	0,912	0,919
	4	0,857	0,939	0,896
	Average	0,868	0,935	0,900

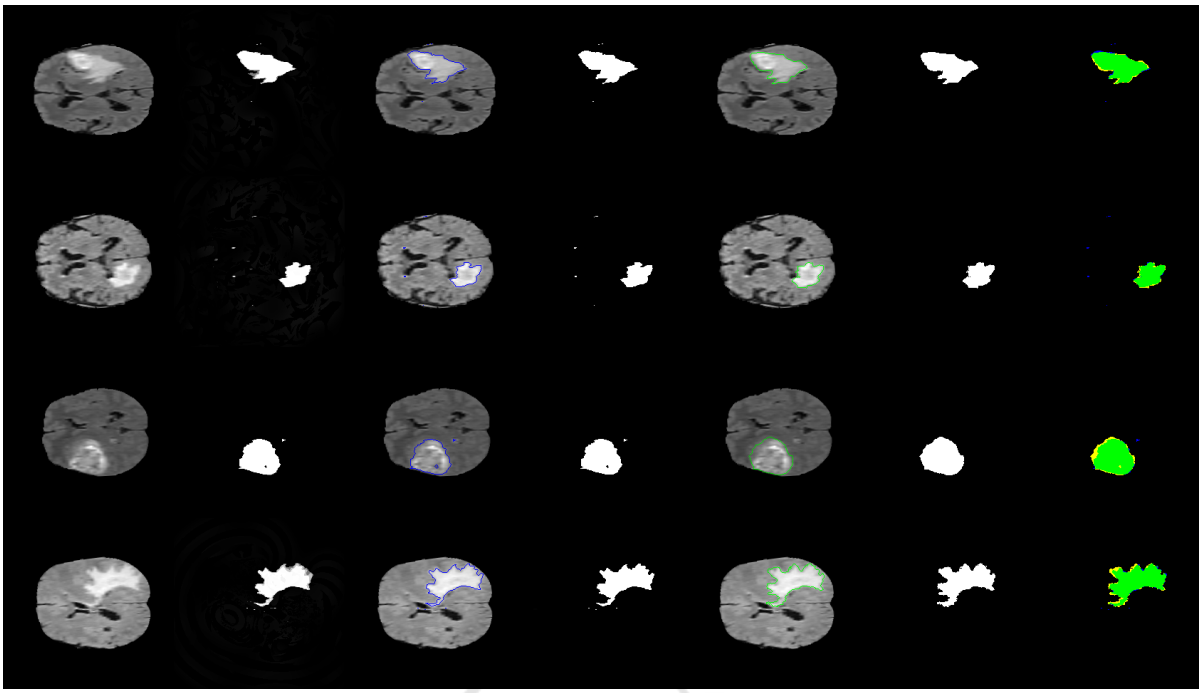

Figure 2: Four FLAIR candidates from BRATS2015 data-set (Menze et al., 2014) (rows). From left to right (columns): original image, output image, perimeter of the segmentation of the output image, output binary mask, perimeter of the ground truth, ground truth segmentation, ground truth and output binary mask overlap (TP-green, TN-black, FP-blue, FN-yellow).

5 CONCLUSIONS

In this work we have presented a new non-local non-convex diffusion model for saliency detection and labeling which has shown to be able to perform a fast foreground detection when it is applied to a FLAIR given image. The results reveal that this method can achieve very high accurate statistics metrics over the ground-truth BRATS2015 data-set (Menze et al., 2014). Also, as a by-product of the model, the solution has, after few iterations, a reduced number of quantized values making simpler the final thresholding step. Such a technique could be improved computationally by observing that the diffusion process combined with the saliency term evolves producing more cartoon like piece-wise constant solutions which can be coded with less number of quantization values while converging to a binary mask. This is related to the absorption-reaction balance in the PDE where absorption is active where the solution is small and the reaction is active where $u \approx 1$. The non-local diffusion properties of the model also allow to detect salient objects which are not spatially close and connected regions (disjoint areas). This can be useful in many other medical images modalities, specially in functional MRI (fMRI). Non-convex properties, meanwhile, promote *sparse* non-local gradient, pushing the solution to a cartoon piece-wise constant image. Both characteristics combined with our proposed concave energy term results in a promising accurate and fast technique suitable to be applied to FLAIR images and others MRI modalities.

ACKNOWLEDGMENTS

This research has been partially supported by the Spanish Government research funding ref. MINECO/FEDER TIN2015-69542-C2-1 and the Banco de Santander and Universidad Rey Juan Carlos Funding Program for Excellence Research Groups ref. Computer Vision and Image Processing (CVIP).

REFERENCES

Ambrosio, L., Fusco, N., and Pallara, D. (2000). *Functions of bounded variation and free discontinuity problems*. Oxford university press.

Andreu-Vaillo, F., Mazón, J. M., Rossi, J. D., and Toledo-Melero, J. J. (2010). *Nonlocal diffusion problems*, volume 165. American Mathematical Society.

Aubert, G., Aujol, J.-F., and Blanc-Féraud, L. (2005). Detecting codimensiontwo objects in an image with

ginzburg-landau models. *International Journal of Computer Vision*, 65(1-2):29–42.

Aubert, G. and Kornprobst, P. (2006). *Mathematical problems in image processing: partial differential equations and the calculus of variations*, volume 147. Springer Science & Business Media.

Banerjee, S., Mitra, S., Shankar, B. U., and Hayashi, Y. (2016). A novel gbm saliency detection model using multi-channel mri. *PloS one*, 11(1):e0146388.

Bylinskii, Z., Judd, T., Borji, A., Itti, L., Durand, F., Oliva, A., and Torralba, A. Mit saliency benchmark.

Chambolle, A. (2004). An algorithm for total variation minimization and applications. *Journal of Mathematical imaging and vision*, 20(1-2):89–97.

Chambolle, A. and Lions, P.-L. (1997). Image recovery via total variation minimization and related problems. *Numerische Mathematik*, 76(2):167–188.

Charbonnier, P., Blanc-Féraud, L., Aubert, G., and Barlaud, M. (1997). Deterministic edge-preserving regularization in computed imaging. *IEEE Transactions on image processing*, 6(2):298–311.

Gilboa, G. and Osher, S. (2008). Nonlocal operators with applications to image processing. *Multiscale Modeling & Simulation*, 7(3):1005–1028.

Harel, J., Koch, C., and Perona, P. (2006). Graph-based visual saliency. In *Advances in neural information processing systems*, pages 545–552.

Hintermüller, M. and Wu, T. (2014). A smoothing descent method for nonconvex tvˆ q-models. In *Efficient Algorithms for Global Optimization Methods in Computer Vision*, pages 119–133. Springer.

Li, M., Zhan, Y., and Zhang, L. (2013). Nonlocal variational model for saliency detection. *Mathematical Problems in Engineering*, 2013.

Liu, R., Cao, J., Lin, Z., and Shan, S. (2014). Adaptive partial differential equation learning for visual saliency detection. In *Proceedings of the IEEE Conference on Computer Vision and Pattern Recognition*, pages 3866–3873.

Liu, Z., Meur, L., and Luo, S. (2013). Superpixel-based saliency detection. In *2013 14th International Workshop on Image Analysis for Multimedia Interactive Services (WIAMIS)*, pages 1–4. IEEE.

Menze, B., Jakab, A., Bauer, S., Kalpathy-Cramer, J., Farahani, K., Kirby, J., Burren, Y., Porz, N., Slotboom, J., Wiest, R., Lanczi, L., Gerstner, E., Weber, M.-A., Arbel, T., Avants, B., Ayache, N., Buendia, P., Collins, L., Cordier, N., Corso, J., Criminisi, A., Das, T., Delingette, H., Demiralp, C., Durst, C., Dojat, M., Doyle, S., Festa, J., Forbes, F., Geremia, E., Glocker, B., Golland, P., Guo, X., Hamamci, A., Iftekharuddin, K., Jena, R., John, N., Konukoglu, E., Lashkari, D., Antonio Mariz, J., Meier, R., Pereira, S., Precup, D., Price, S. J., Riklin-Raviv, T., Reza, S., Ryan, M., Schwartz, L., Shin, H.-C., Shotton, J., Silva, C., Sousa, N., Subbanna, N., Szekely, G., Taylor, T., Thomas, O., Tustison, N., Unal, G., Vasseur, F., Wintermark, M., Hye Ye, D., Zhao, L., Zhao, B., Zikic, D., Prastawa, M., Reyes, M., and Van Leemput, K. (2014). The Multimodal Brain Tumor Image Segmentation Benchmark (BRATS). *IEEE Transactions on Medical Imaging*, page 33.

Rudin, L. I., Osher, S., and Fatemi, E. (1992). Nonlinear total variation based noise removal algorithms. *Physica D: Nonlinear Phenomena*, 60(1):259–268.

Rueda, A., González, F., and Romero, E. (2013). Saliency-based characterization of group differences for magnetic resonance disease classification. *Dyna*, 80(178):21–28.

Samson, C., Blanc-Féraud, L., Aubert, G., and Zerubia, J. (1998). *Image classification using a variational approach*. PhD thesis, INRIA.

Thota, R., Vaswani, S., Kale, A., and Vydyanathan, N. (2016). Fast 3d salient region detection in medical images using gpus. In *Machine Intelligence and Signal Processing*, pages 11–26. Springer.

Tomasi, C. and Manduchi, R. (1998). Bilateral filtering for gray and color images. In *Computer Vision, 1998. Sixth International Conference on*, pages 839–846. IEEE.

Wang, Y., Liu, R., Song, X., and Su, Z. (2014). Saliency detection via nonlocal l_ {0} minimization. In *Asian Conference on Computer Vision*, pages 521–535. Springer.

Weickert, J. (1998). *Anisotropic diffusion in image processing*, volume 1. Teubner Stuttgart.

Yang, Q., Tan, K.-H., and Ahuja, N. (2009). Real-time o (1) bilateral filtering. In *Computer Vision and Pattern Recognition, 2009. CVPR 2009. IEEE Conference on*, pages 557–564. IEEE.

Zhan, Y. (2011). The nonlocal-laplacian evolution for image interpolation. *Mathematical Problems in Engineering*, 2011.